JACS
JOURNAL OF THE AMERICAN CHEMICAL SOCIETY

Article

pubs.acs.org/JACS

Through-Space Charge Interaction Substituent Effects in Molecular Catalysis Leading to the Design of the Most Efficient Catalyst of CO_2-to-CO Electrochemical Conversion

Iban Azcarate, Cyrille Costentin,* Marc Robert,* and Jean-Michel Savéant*

Laboratoire d'Electrochimie Moléculaire, Unité Mixte de Recherche Université - CNRS No. 7591, Université Paris Diderot, Sorbonne Paris Cité, Bâtiment Lavoisier, 15 rue Jean de Baïf, 75205 Paris Cedex 13, France

Supporting Information

ABSTRACT: The starting point of this study of through-space substituent effects on the catalysis of the electrochemical CO_2-to-CO conversion by iron(0) tetraphenylporphyrins is the linear free energy correlation between through-structure electronic effects and the iron(I/0) standard potential that we established separately. The introduction of four positively charged trimethylanilinium groups at the para positions of the tetraphenylporphyrin (TPP) phenyls results in an important positive deviation from the correlation and a parallel improvement of the catalytic Tafel plot. The assignment of this catalysis boosting effect to the Coulombic interaction of these positive charges with the negative charge borne by the initial Fe^0-CO_2 adduct is confirmed by the negative deviation observed when the four positive charges are replaced by four negative charges borne by sulfonate groups also installed in the para positions of the TPP phenyls. The climax of this strategy of catalysis boosting by means of Coulombic stabilization of the initial Fe^0-CO_2 adduct is reached when four positively charged trimethylanilinium groups are introduced at the ortho positions of the TPP phenyls. The addition of a large concentration of a weak acid—phenol—helps by cleaving one of the C–O bonds of CO_2. The efficiency of the resulting catalyst is unprecedented, as can be judged by the catalytic Tafel plot benchmarking with all presently available catalysts of the electrochemical CO_2-to-CO conversion. The maximal turnover frequency (TOF) is as high as 10^6 s^{-1} and is reached at an overpotential of only 220 mV; the extrapolated TOF at zero overpotential is larger than 300 s^{-1}. This catalyst leads to a highly selective formation of CO (practically 100%) in spite of the presence of a high concentration of phenol, which could have favored H_2 evolution. It is also very stable, showing no significant alteration after more than 80 h of electrolysis.

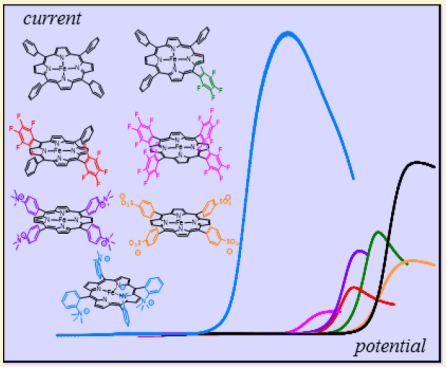

INTRODUCTION

We analyze in detail elsewhere[1] how substituents exerting a through-structure electronic effect influence the thermodynamics and kinetics of the catalysis of the electrochemical CO_2-to-CO conversion, taking as an example a series of phenyl-substituted iron(I/0) tetraphenylporphyrins. Catalytic Tafel plots (Figure 1) relating the electrochemical turnover frequency (TOF) to the overpotential, $\eta = (E^0_{t,r} - E)$, with $E^0_{t,r} = E^0_{CO_2/CO,DMF} = -0.74$ V vs SHE (see the Supporting Information (SI)), were used to gauge the substituent effects.

They also allowed the rational benchmarking of the catalysts independently of the cell characteristics for the electrochemical CO_2-to-CO-conversion,[2a] but also for other reactions.[2b] Two conflicting trends appear for these through-structure effects: positive shifts of the catalyst's standard potential, entailing a favorable decrease of the overpotential η, are accompanied by unfavorable decreases of TOF_{max} (and *vice versa*). These two factors obey a linear free energy relationship in which the standard potential of the $Fe^{I/0}$ couple (E^0_{cat}) may serve as a thermodynamic index measuring the standard free energy of each substituent. This is the main finding of ref 1 that will be used in the following discussion, rather than the otherwise important detailed analysis of the substituent effects on each step of the four-step process it also provided. The relevant results for FeTPP and the three perfluorophenylporphyrins (Chart 1) are recalled in Figure 2 in the form of both catalytic Tafel plots (Figure 2a) and linear correlation between $(RT \ln 10/F) \log k_{cat}$ and E^0_{cat} (Figure 2b).

In seeking to solubilize in water a catalyst of the same family, we were led to synthesize and test the porphyrin designed by iron tetra(*p*-*N*,*N*,*N*-trimethylanilinium)porphyrin (abbreviated as Fe-*p*-TMA, Chart 2), which bears four positively charged trimethylammonio substituents at the para positions of the phenyl rings. We thus obtained a catalyst that is not only soluble in water but that also has proved very effective, to the point of being integrated, after deposition on the cathode surface, into an operational electrolyzer.[3]

The question that then naturally arises is whether these charged substituents may or may not exert the same through-structure inductive effect as the Chart 1 porphyrins, the

Received: July 7, 2016
Published: November 11, 2016

DOI: 10.1021/jacs.6b07014
J. Am. Chem. Soc. 2016, 138, 16639–16644

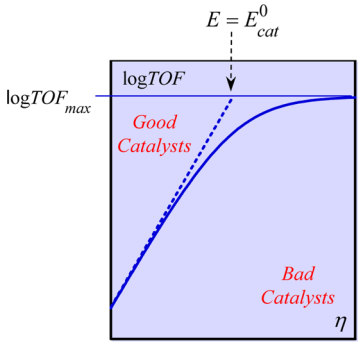

$$TOF = \frac{k_{cat}}{1+\exp\left[\frac{F}{RT}\left(E-E^0_{cat}\right)\right]},\quad \eta = E^0_{tr} - E$$

$$TOF = \frac{TOF_{max}}{1+\exp\left[\frac{F}{RT}\left(E^0_{tr}-E^0_{cat}\right)\right]\times\exp\left(-\frac{F}{RT}\eta\right)}$$

E: electrode potential

E^0_{tr}: standard potential of the target reaction

E^0_{cat}: catalyst standard potential

C^0_{cat}: catalyst concentration

Figure 1. Catalytic Tafel plot.

Chart 1

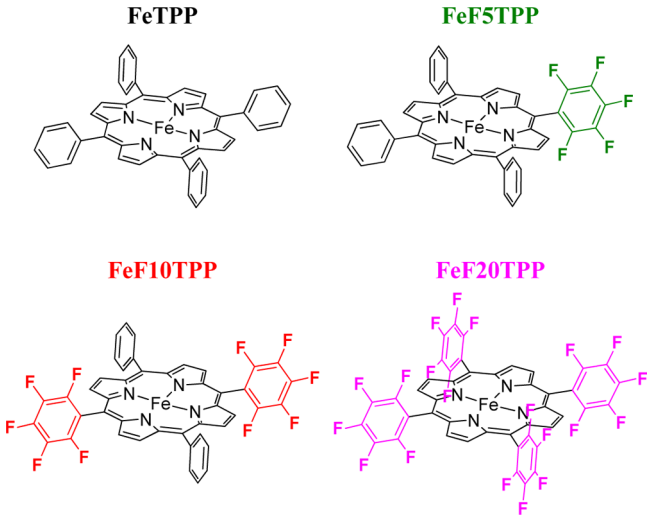

characteristics of which are recalled in Figure 2. The existence of a specific effect of the positive charges borne by the four trimethylanilinium groups was then checked by comparison with a porphyrin bearing four negative charges (Fe-*p*-PSULF in Chart 2), which shows an opposite deviation from the $(RT\ln 10/F)\log k_{cat}$ and E^0_{cat} correlation.

These charged substituents at the para positions of the phenyl rings are quite distant from the iron catalytic center. Thus, the specific Coulombic effect, even if significant, is not expected to be very strong. This is the reason that we prepared and tested another tetra(trimethylanilinium)porphyrin, which bears the same four trimethylammonio groups but at the ortho positions of the phenyl groups (Fe-*o*-TMA). Compared to Fe-*p*-TMA, the Coulombic interaction effects in Fe-*o*-TMA are expected to be much stronger because of the closer proximity of the charges to the reacting center. This is indeed what

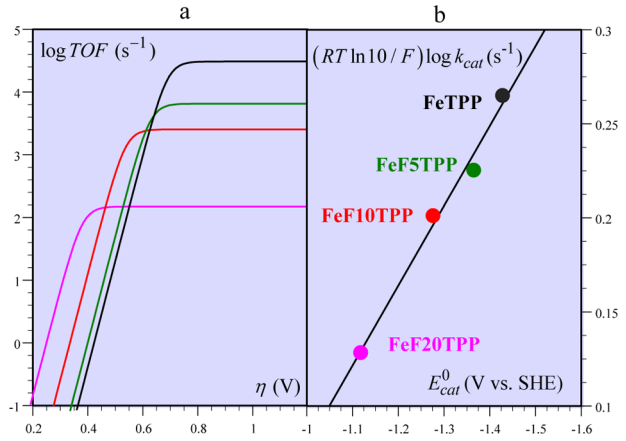

Figure 2. (a) Catalytic Tafel plots of the porphyrins of Charts 1 for [PhOH] = 3 M. (b) Correlation between TOF_{max} = k_{cat} and E^0_{cat}, recalling the through-structure substituent effect. The color code is the same as in Chart 1.

Chart 2

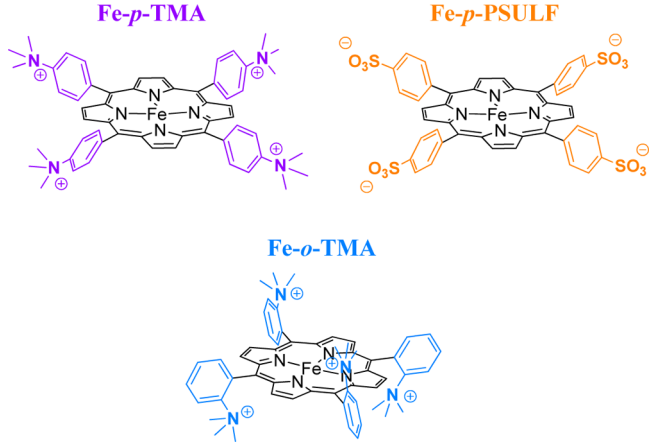

happens, as will be detailed in the next sections, making this molecule a considerably better catalyst for the electrochemical CO_2-to-CO-conversion than all molecules that have been tested so far. Particular care was exerted to prepare this molecule, to analyze its cyclic voltammetric responses so as to obtain its catalytic Tafel plot and its representative point in the $(RT\ln 10/F)\log k_{cat}$ vs E^0_{cat} correlation. This catalyst also performs remarkably in terms of CO/H_2 selectivity and in terms of stability over long-time preparative-scale electrolyses.

RESULTS AND DISCUSSION

Figure 3 shows the $Fe^{I/0}$ cyclic voltammetric responses obtained with the eight porphyrins of Charts 1 and 2 under 1 atm CO_2 in the presence of 3 M phenol. It immediately appears, before any treatment of the raw data, that the Fe-*o*-TMA is a far much better catalyst than any other molecules in the series, in terms of both current and potential. We will return to this point after the raw data have been treated to see how the substituent effects in the Chart 2 porphyrins fall in line, or not, with the through-structure electronic effects detected and rationalized with the Chart 1 substituents.[1]

As seen in Figure 4, the cyclic voltammetry (CV) response of the three charged porphyrins of Chart 2 is similar to that of the neutral porphyrins we have studied separately.[1] As already observed,[3a] the electro-withdrawing inductive effect of the four

DOI: 10.1021/jacs.6b07014
J. Am. Chem. Soc. 2016, 138, 16639−16644

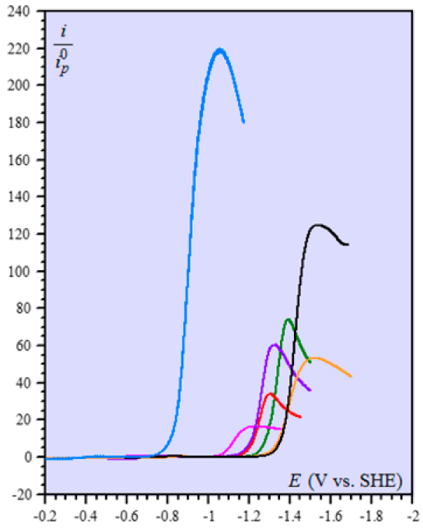

Figure 3. Cyclic voltammetry of Fe-*o*-TMA (light blue), FeF20TPP (magenta), FeF10TPP (red), Fe-*p*-TMA (purple), FeF5TPP (green), FeTPP (black), and Fe-*p*-PSULF (orange) in the potential domain of the catalytic CO_2 reduction wave in DMF + 0.1 M *n*-Bu_4NPF_6 + 0.1 M H_2O + 3 M PhOH, at 0.1 V/s under 1 atm CO_2 (catalyst conc.: 1 mM). The current, *i*, is normalized against the peak current of the reversible one-electron Fe^{II}/Fe^{I} reversible wave, i_p^0, obtained at the same scan rate (0.1 V/s).

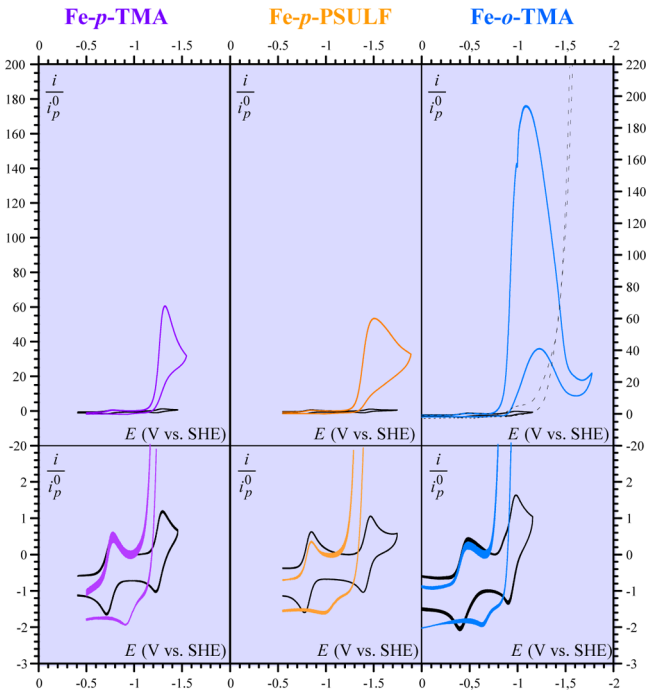

Figure 4. Cyclic voltammetry of the substituted iron porphyrins of Chart 2 (conc.: 1 mM) in DMF + 0.1 M *n*-Bu_4NPF_6 + 0.1 M H_2O at 0.1 V/s under argon (black) and under 1 atm CO_2 in the presence of 3 M PhOH. The dotted black line in the top right of the figure is the CV response observed under 1 atm Ar in the presence of 3 M PhOH. The bottom figures are blow-ups of the upper figures, showing the formation of CO on the reverse scan (see text).

trimethylanilinium groups at the para positions of Fe-*p*-TMA is responsible for a quite significant shift of E^0_{cat} toward positive potential (E^0_{cat} = −1.263 V vs SHE, 165 mV more positive than with FeTPP). This effect is even stronger when the trimethylanilinium groups are placed at the ortho positions. E^0_{cat}(Fe-*o*-TMA) = −0.944 V vs SHE (484 mV more positive than with FeTPP), which is the most positive potential ever reported for an iron porphyrin CO_2-reduction catalyst. On the other hand, the sulfonate groups of Fe-*p*-PSULF exert almost no effect on the standard potential of the catalyst (E^0_{cat} = −1.428 V vs SHE).

The formation of CO is clearly attested by the observation of a cathodic shift of the Fe^{I}/Fe^{II} re-oxidation wave on the reverse scan in the CV catalytic responses of the three porphyrins of Chart 2. As with the other porphyrins, it matches what can be observed in the CV of the Fe^{II}/Fe^{I} couple in the presence of CO. We will confirm the quasi-exclusive formation of CO during long-term preparative-scale electrolyses.

It is noticed (Figures 3 and 4) that the current−potential responses of the three porphyrins of interest show peaks instead of the plateaus expected for fast catalytic processes. As analyzed in detail elsewhere,[4] this is due to the interference of secondary phenomena such as substrate or co-substrate consumption, inhibition by product, and possibly other phenomena that all increase with the charge passed. One way of fighting the interference of such phenomena is to raise the scan rate, and thereby decrease the charge passed, so as to get back to an S-shaped current potential response and derive the rate constant from the ensuing current plateau.

This is the treatment that has been applied to the raw CV data as shown in Figure 5. It is worth noting, *en passant*, that the scan rates required to reach an S-shaped CV response are, as expected, larger for stronger catalysis (in increasing order: Fe-*p*-PSULF, Fe-*p*-TMA, Fe-*o*-TMA).

The values of k_{cat} required to establish the catalytic Tafel plots and the $(RT \ln 10/F)\log k_{cat}$ vs E^0_{cat} for these three porphyrins may then be derived from the plateau current values, using the following equations. For the catalytic current plateau, $i_{pl} = FSC^0_{cat}\sqrt{D_{cat}}\sqrt{2k_{cat}}$, and for the one-electron diffusion current at 0.1 V/s, $i_p^0 = FS \times 0.446 \times C^0_{cat}\sqrt{D_{cat}}\sqrt{\frac{Fv(=0.1\ \mathrm{V/s})}{RT}}$. Using the ratio

$$\frac{i_{pl}}{i_p^0} = 2.24 \times \sqrt{\frac{2k_{cat}}{0.1}\frac{RT}{F}}$$

avoids determining *S* (electrode surface area), C^0_{cat} (concentration of the catalyst), and D_{cat} (diffusion coefficient of the catalyst). Thus,

$$k_{cat} = \left(\frac{i_{pl}}{i_p^0}\right)^2 \frac{0.1}{2.24^2}\frac{F}{2RT}$$

The values of k_{cat} thus obtained were then used to locate the catalytic Tafel plots of the three Chart 2 porphyrins (Figure 6a) and to introduce the corresponding data points in the $(RT \ln 10/F)\log k_{cat}$ vs E^0_{cat} correlation diagram (Figure 6b).

A through-space effect clearly appears for Fe-*p*-TMA insofar as its representative point stands above the through-structure correlation line (purple dot in Figure 6b). That this effect results from the positive charges borne by the substituents is confirmed by the observation that the introduction of negative charges in similar positions produces the reverse effect (Figure 6b). Although clearly present, these effects are necessarily small since the charges are rather distant from the reacting center, viz., the initial adduct between CO_2 and the iron(0) complex.

These observations encouraged us to introduce positively charged substituents closer to the reacting center in spite of the

DOI: 10.1021/jacs.6b07014
J. Am. Chem. Soc. 2016, 138, 16639−16644

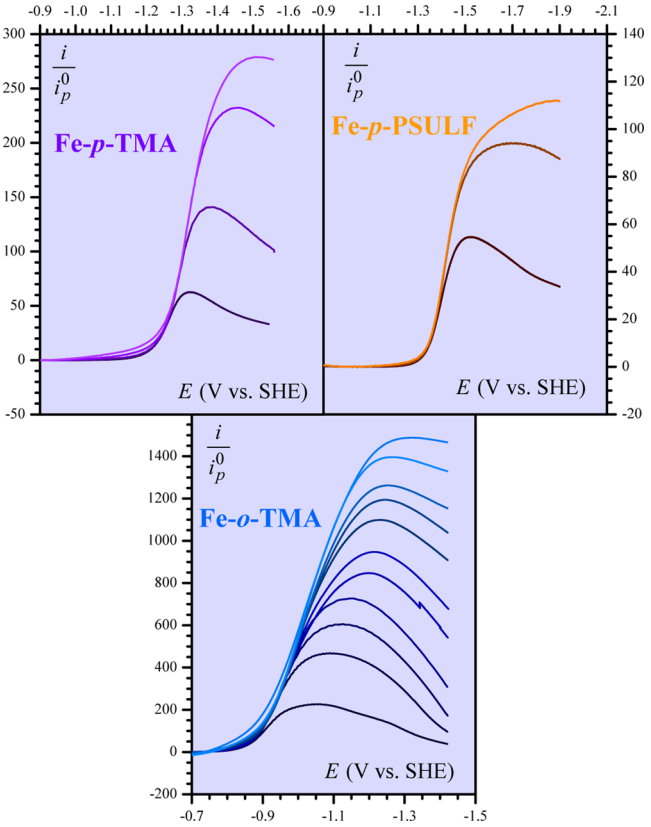

Figure 5. Elimination of the secondary phenomena by raising the scan rate (see text). Cyclic voltammetry of the substituted iron porphyrins of Chart 2 (conc.: 1 mM) in DMF + 0.1 M NBu_4PF6 + 0.1 M H_2O under 1 atm CO_2 in the presence of 3 M PhOH at the following scan rates (V/s), from bottom to top: Fe-*p*-TMA: 0.1, 1, 5, and 10; Fe-*p*-PSULF: 0.1, 1, and 2; Fe-*o*-TMA: 0.1, 0.5, 1, 2, 6, 10, 20, 30, 48, 96, and 115. The current, *i*, is normalized against the peak current of the reversible one-electron Fe^{II}/Fe^{I} reversible wave, i_p^0, obtained at 0.1 V/s.

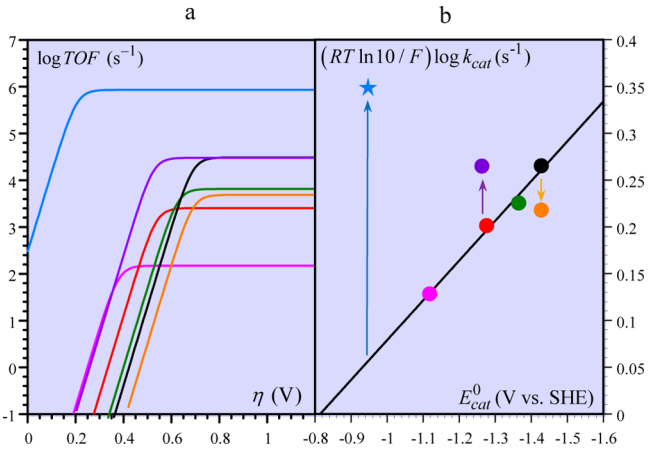

Figure 6. (a) Catalytic Tafel plots of the porphyrins of Charts 1 and 2. (b) Correlation between $TOF_{max} = k_{cat}$ and E^0_{cat}, recalling the through-structure substituent effect and showing the Coulombic interaction effects of positively and negatively charged substituents, including the huge gain in reactivity and overpotential brought about by positively charged substituents when located at the ortho positions of the phenyl rings. Color code: Fe-*o*-TMA, light blue; FeF20TPP, magenta; FeF10TPP, red; Fe-*p*-TMA, purple; FeF5TPP, green; FeTPP, black; and Fe-*p*-PSULF, orange.

expected synthetic difficulties related to steric congestion of this type of substituted iron porphyrin. The result, Fe-*o*-TMA, proved to be the best catalyst of the whole iron porphyrin series, with considerable gains in terms of overpotential and of TOF, as can be seen in Figure 6. The maximal TOF is as high as 10^6 s^{-1}, and the extrapolated TOF at zero overpotential is larger than 300 s^{-1}.

The reason for this leap forward is most likely the stabilization of the initial Fe(0)−CO_2 adduct by the interaction of the negative charge borne by the oxygens of CO_2 in this adduct with the nearby positive charges borne by the trimethylanilinium substituents on the porphyrin phenyls. The presence of phenol in large concentration then helps the proton-assisted reductive cleavage of one of the carbon−oxygen bonds of CO_2 (see Scheme 1 in ref 1). This is a particularly striking example of the power of close-distance through-space interactions in boosting catalysis. Another type of close-distance through-space interactions has already been implemented to boost CO_2 reduction catalysis, albeit with a lesser efficiency, namely the introduction of ortho phenol groups on the porphyrin phenyls (see Chart 3),[4c] in which stabilization of the

Chart 3

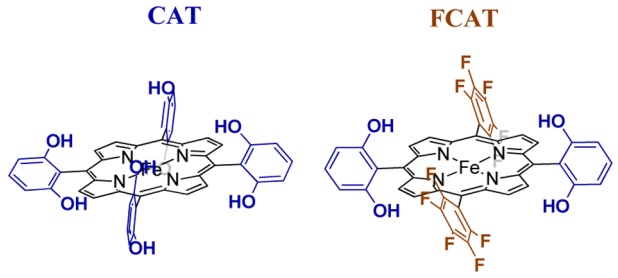

initial Fe^0−CO_2 adduct is achieved by means of H-bonding rather than by means of Coulombic interactions as in the present case. Comparison between the Coulombic interaction and H-bond interaction series is shown in Figure 7, as well as that with the best examples of molecular catalysts that can be found in the literature. It appears that Fe-*o*-TMA is, to a large extent, the most efficient of the whole series in terms of catalytic Tafel plots.

The next step was to look at the selectivity and durability of the catalyst at the preparative scale. Figure 8 shows the Faradaic yields in CO and H_2 for Fe-*o*-TMA and Fe-*p*-TMA over 7 h of electrolysis time. In both cases, the catalysts appear stable, and the CO-vs-H_2 selectivity is excellent. Actually, a slight improvement in the selectivity is observed for Fe-*o*-TMA, which presents a CO selectivity of 100%, compared to a CO selectivity of 93% for Fe-*p*-TMA. The durability of Fe-*o*-TMA was evaluated by performing a series of four consecutive electrolyses with the same catalytic solution at an overpotential of 220 mV (at which the TOF is 10^6 s^{-1}), over a total of 84 h. The first and fourth electrolyses were done in a glassy carbon crucible, while the second and third ones were performed at a Hg pool. From the almost linear evolution of the charge vs time (Figure 9a), it was concluded that CO_2 was continuously reduced, with no noticeable sign of catalyst degradation. Note that some PhOH was added to the catalytic solution after each electrolysis to keep a sufficient concentration and maintain the activity. The selectivity toward CO remained equal to 100% during the whole experiment, regardless of the nature of the working electrode. This good selectivity falls in line with the

DOI: 10.1021/jacs.6b07014
J. Am. Chem. Soc. 2016, 138, 16639−16644

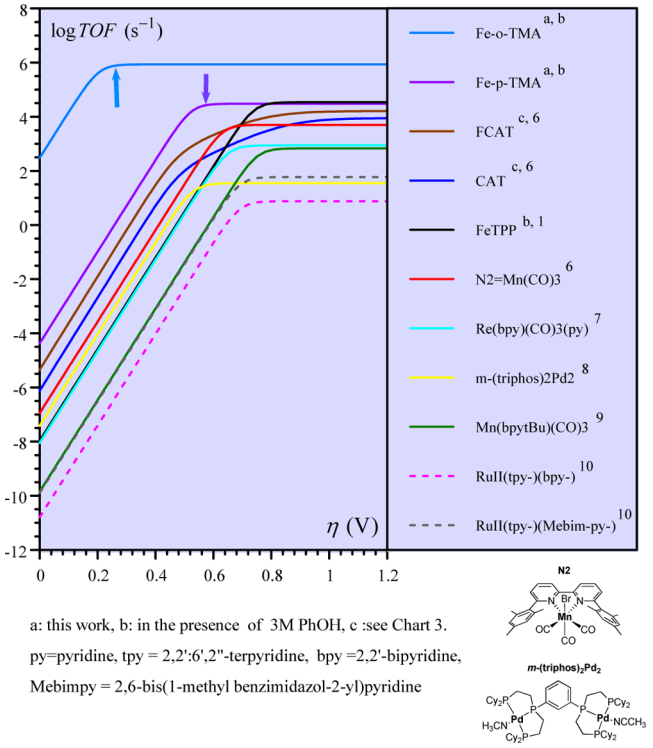

Figure 7. Benchmarking of the main molecular catalysts of the CO_2-to-CO electrochemical conversion in DMF or acetonitrile[5−10] by means of their catalytic Tafel plots. The vertical arrows indicate the overpotential values at which the electrolyses were carried out (see text and Figure 8).

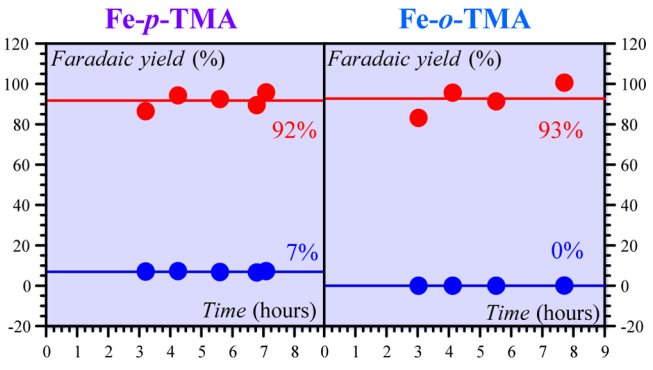

Figure 8. Preparative-scale electrochemical CO_2-to-CO conversion catalyzed by Fe-*p*-TMA (at an overpotential of 450 mV, purple vertical arrow in Figure 6) and Fe-*o*-TMA (at an overpotential of 220 mV, light blue vertical arrow in Figure 6) in DMF + 0.1 M NBu_4PF_6 + 0.1 M H_2O under 1 atm CO_2 in the presence of 3 M PhOH (catalyst conc.: 0.5 mM). CO (red dots) and H_2 (blue dots) Faradaic yields.

CV responses shown in the top right of Figure 4, where it is seen that the current observed under Ar in the presence of 3 M phenol is considerably less that the catalytic current observed in the presence of CO_2.

A control electrolysis performed with a fresh solution containing no catalyst, with a used glassy carbon crucible, demonstrates that no iron catalyst was deposited on the electrode (see SI). The stability of Fe-*o*-TMA was also monitored by means of UV−vis spectroscopy and CV (see SI, Figure S1). While some shifts in the Soret band and in the $Fe^{III/II/I}$ CV waves resulting from the products' formation are observed, the catalytic $Fe^{I/0}$ catalytic CV wave remains remarkably stable.

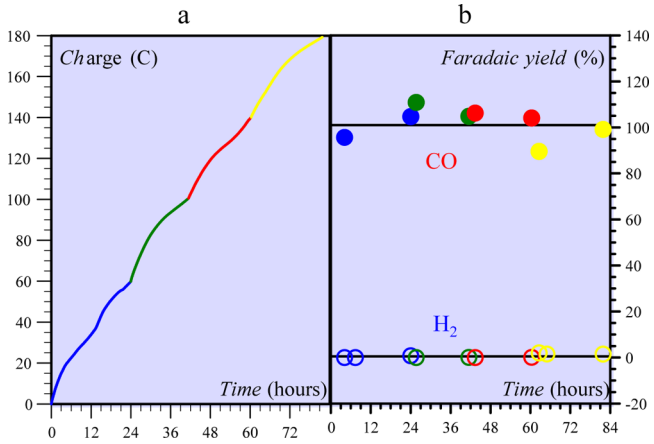

Figure 9. Long run (84 h) preparative-scale electrochemical CO_2-to-CO conversion catalyzed by Fe-*o*-TMA (at an overpotential of 220 mV, light blue vertical arrow in Figure 6) in DMF + 0.1 M nBu_4NPF_6 + 0.1 M H_2O under 1 atm CO_2 in the presence of 3 M PhOH (catalyst conc.: 0.5 mM). (a) Charge evolution and (b) Faradaic yields (CO, full circles; H_2, open circles) during 24 h on a carbon electrode (blue), then 18 h on a mercury electrode (green), then during a second 18 h period again on a mercury electrode (red), and finally during another 24 h period on a carbon electrode (yellow).

CONCLUSIONS

Through-space substituent effects on the catalysis of the electrochemical CO_2-to-CO conversion by iron(0) tetraphenylporphyrins has been for the first time investigated and evidenced by the introduction of four positively charged trimethylanilinium groups at the para positions of the TPP phenyls (Fe-*p*-TMA). The assignment of this catalysis boosting effect to the Coulombic interaction of these positive charges with the negative charges borne by the initial Fe^0-CO_2 adduct has been further confirmed by the negative catalytic effect observed when the four positive charges in Fe-*p*-TMA are replaced by four negative charges provided by four sulfonate groups installed at the para positions of the TPP phenyls (Fe-*p*-PSULF). Optimization of the catalysis by means of Coulombic stabilization of the initial Fe^0-CO_2 adduct was reached when four positively charged trimethylanilinium groups were introduced at the ortho positions of the TPP phenyls (Fe-*o*-TMA). The exceptional efficiency of the resulting catalyst is unprecedented, with maximal TOF as high as 10^6 s^{-1}, reached at a low overpotential of 220 mV. The selectivity for CO production is close to 100%, while the catalyst appears extremely stable upon long-term electrolysis, with no significant alteration for more than 3.5 days.

EXPERIMENTAL SECTION

An original synthetic pathway has been developed to synthesize Fe-*o*-TMA. The synthesis of the other Fe porphyrins in Chart 2 is described in the SI, as well as information concerning the other chemicals and the instrumentation and procedure for CV. Fe-*o*-TMA was prepared according to the flow diagram in Chart 4 from the reaction of 2-nitrobenzaldehyde and pyrrole in five steps with 9% overall yield. First, tetra-*o*-nitrophenylporphyrine (**1**) was prepared by condensation of 2-nitrobenzaldehyde with pyrrole in refluxing acetic acid.[11] Porphyrin **1** was then reduced by $SnCl_2$ in concentrated HCl to give the tetra-*o*-aminophenylporphyrine (**2**) as a statistic mixture of four atropisomers (see inset in Chart 4 for a schematic representation of the

DOI: 10.1021/jacs.6b07014
J. Am. Chem. Soc. 2016, 138, 16639−16644

Chart 4

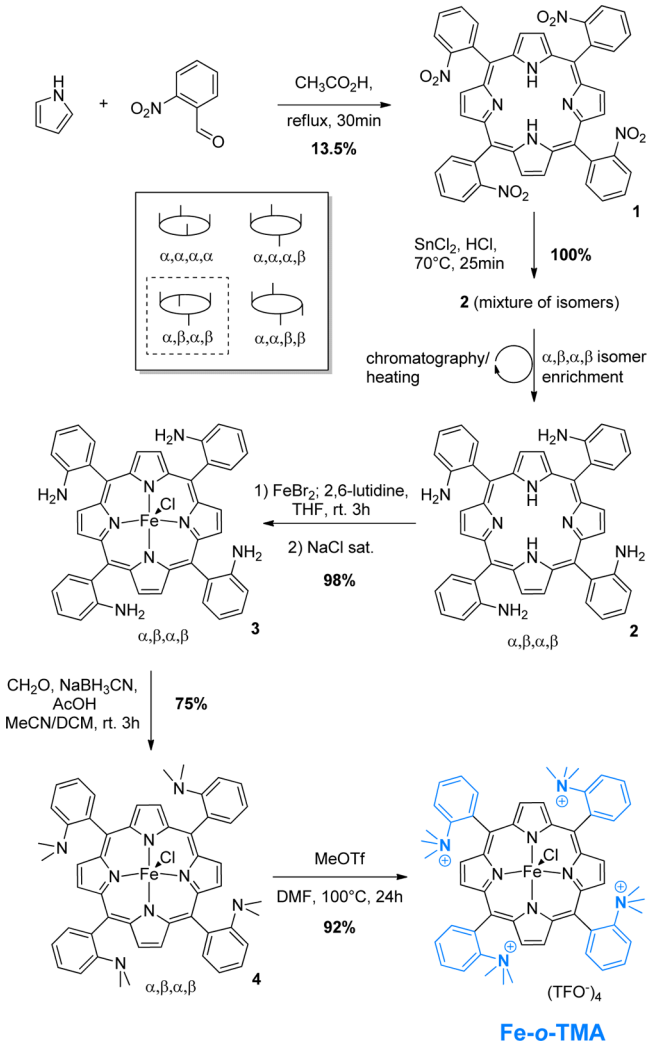

atropisoemers). Column chromatography led to the isolation of pure *α,β,α,β* isomer. The three remaining isomers can be converted to a new statistic mixture of the four atropisomers after refluxing in toluene for an additional 6 h. An almost complete conversion of **2** into the desired *α,β,α,β* isomer can be achieved by repeating this chromatography/heating cycle. Treatment of **2** with $FeBr_2$, followed by reductive amination with formaldehyde and sodium cyanoborohydride, yielded the metalated dimethylamino intermediate **4**. The mild conditions used in these two successive steps allowed the isolation of **4** in a pure *α,β,α,β* configuration.

Finally, porphyrin **4** was quaternized by reaction with a large excess of methyl triflate in hot DMF to yield the desired Fe-*o*-TMA as a triflate salt. Several milder quaternization methods were tried, with no decisive success. It may therefore be that some isomerization occurs, leading to the formation of small amounts of the *α,α,β,β*, *α,α,α,β*, and *α,α,α,α* isomers. Their separation was not attempted since they present similar capabilities to stabilize the initial Fe^0-CO_2 adduct through Coulombic interaction as the *α,β,α,β* isomer. The catalyst was fully characterized by infrared spectroscopy, UV−vis absorbance, elemental analysis, and mass spectrometry (see SI for details).

■ ASSOCIATED CONTENT

Supporting Information

The Supporting Information is available free of charge on the ACS Publications website at DOI: 10.1021/jacs.6b07014.

Experimental details; determination of $E^0_{CO_2/CO}$ according to the solvent and the acids present (PDF)

■ AUTHOR INFORMATION

Corresponding Authors

*cyrille.costentin@univ-paris-diderot.fr
*robert@univ-paris-diderot.fr
*saveant@univ-paris-diderot.fr

Notes

The authors declare no competing financial interest.

■ ACKNOWLEDGMENTS

Partial financial support from the SATT IDF Innov (project 098) is gratefully acknowledged.

■ REFERENCES

(1) Azcarate, I.; Costentin, C.; Robert, M.; Savéant, J. M. *J. Phys. Chem. C* **2016**, DOI: 10.1021/acs.jpcc.6b09947.

(2) (a) Costentin, C.; Robert, M.; Savéant, J.-M. *Acc. Chem. Res.* **2015**, *48*, 2996. (b) Artero, V.; Savéant, J.-M. *Energy Environ. Sci.* **2014**, *7*, 3808.

(3) (a) Costentin, C.; Robert, M.; Savéant, J.-M.; Tatin, A. *Proc. Natl. Acad. Sci. U. S. A.* **2015**, *112*, 6882. (b) Tatin, A.; Comminges, C.; Kokoh, B.; Costentin, C.; Robert, M.; Savéant, J.-M. *Proc. Natl. Acad. Sci. U. S. A.* **2016**, *113*, 5526.

(4) (a) Costentin, C.; Drouet, S.; Robert, M.; Savéant, J.-M. *J. Am. Chem. Soc.* **2012**, *134*, 11235; **2012**, *134*, 19949. (b) Costentin, C.; Drouet, S.; Passard, G.; Robert, M.; Savéant, J.-M. *J. Am. Chem. Soc.* **2013**, *135*, 9023. (c) Costentin, C.; Passard, G.; Robert, M.; Savéant, J.-M. *J. Am. Chem. Soc.* **2014**, *136*, 11821. (d) Costentin, C.; Passard, G.; Savéant, J.-M. *J. Am. Chem. Soc.* **2015**, *137*, 5461.

(5) Costentin, C.; Passard, G.; Robert, M.; Savéant, J.-M. *Proc. Natl. Acad. Sci. U. S. A.* **2014**, *111*, 14990.

(6) Sampson, M. D.; Nguyen, A. D.; Grice, K. A.; Moore, C. E.; Rheingold, A. L.; Kubiak, C. P. *J. Am. Chem. Soc.* **2014**, *136*, 5460.

(7) Wong, K.-Y.; Chung, W.-H.; Lau, C.-P. *J. Electroanal. Chem.* **1998**, *453*, 161.

(8) Raebiger, J. W.; Turner, J. W.; Noll, B. C.; Curtis, C. J.; Miedaner, A.; Cox, B.; DuBois, D. L. *Organometallics* **2006**, *25*, 3345.

(9) Smieja, J. M.; Sampson, M. D.; Grice, K. A.; Benson, E. E.; Froehlich, J. D.; Kubiak, C. P. *Inorg. Chem.* **2013**, *52*, 2484.

(10) Chen, Z.; Chen, C.; Weinberg, D. R.; Kang, P.; Concepcion, J. J.; Harrison, D. P.; Brookhart, M. S.; Meyer, T. J. *Chem. Commun.* **2011**, *47*, 12607.

(11) Collman, J. P.; Gagne, R. R.; Reed, C.; Halbert, T. R.; Lang, G.; Robinson, W. T. *J. Am. Chem. Soc.* **1975**, *97*, 1427.

DOI: 10.1021/jacs.6b07014
J. Am. Chem. Soc. 2016, 138, 16639−16644